Bull. Chem. Soc. Jpn., 75, 943–948 (2002)

Transient Resonance Raman Spectroscopy and Density Functional Theory Investigation of Iso-Dibromoacetic Acid Photoproduct Produced From Ultraviolet Photolysis of Dibromoacetic Acid in the Solution Phase

Yun-Liang Li, Dongqi Wang, and David Lee Phillips*

Department of Chemistry, University of Hong Kong, Pokfulam Road, Hong Kong

(Received August 29, 2001)

We present transient resonance Raman spectra and density functional theory calculations that indicate the iso-dibromoacetic acid (Br–BrCHCOOH) species can be produced in noticeable amounts following ultraviolet photolysis of dibromoacetic acid in cyclohexane solution. We compare the properties of the iso-dibromoacetic acid species to those previously found for the related iso-dibromomethane species. We briefly discuss the potential utility of using iso-dibromoacetic acid in cyclopropanation reactions to make substituted cyclopropane products.

Polyhalomethanes like CH_2I_2, CH_2Br_2, $CHBr_3$, CH_2IBr and others have been seen in the atmosphere and are believed to be significant sources of reactive halogens in the atmosphere.[1–6] Polyhalomethanes can also be used in synthetic chemistry to perform cyclopropanation reactions.[7–10] For instance, ultraviolet excitation of CH_2I_2 (and to a lesser extent CH_2Br_2) in the presence of olefins leads to efficient formation of a cyclopropanated product.[7–10] We have recently observed formation of isopolyhalomethane photoproduct species after ultraviolet photolysis of a number of different polyhalomethanes in room temperature solutions.[11–18] Comparison of femtosecond time-resolved absorption spectroscopy experiments[19–22] and picosecond time-resolved resonance Raman spectroscopy experiments[16,17,23] for several dihalomethanes suggests that the isopolyhalomethane photoproduct species is initially formed vibrationally hot following geminate recombination of the CH_2X and X or Y (where X, Y are I, Br or Cl halogen atoms) fragments within the solvent cage.[16,17,19–23] Isopolyhalomethanes have also been previously observed in low temperature matrix isolation experiments following ultraviolet photolysis of polyhalomethanes.[24–27]

Recent density functional theory (DFT) calculations found that the isodiiodomethane (CH_2I–I) species easily reacts with ethylene to produce a cyclopropane product and iodine molecule leaving group via a single-step reaction with a barrier height of about 2.9 kcal/mol.[28] However, the CH_2I radical and CH_2I^+ cation species were found to react with ethylene via a two-step reaction process to make a cyclopropane product with large barriers to reaction for the rate determining step.[28] These DFT calculation results and comparison to previous experimental results suggest that isodiiodomethane (CH_2I–I) is the carbenoid species mainly responsible for the cyclopropanation reaction with olefins via ultraviolet excitation of CH_2I_2. Recent time-resolved resonance Raman spectroscopy experiments found that CH_2I–I reacts with cyclohexene on the 5–10 ns time-scale to produce an iodine molecule leaving group that almost immediately forms an I_2 : cyclohexene complex[29] under conditions that Blomstrom, Herbig and Simmons found substantial conversion of cyclohexene into its cyclopropanated product norcarane.[7] This also provides further support for CH_2I–I being the carbenoid or methylene transfer agent responsible for cyclopropanation of olefins via ultraviolet photolysis of CH_2I_2. Further DFT computational results also indicate other isodihalomethane species can be carbenoid species with potential use for cyclopropanation reactions.[30]

We are beginning to explore whether molecular systems larger than polyhalomethanes are also able to form similar isomer species following ultraviolet photolysis in liquid solutions. Such molecular systems may be useful to do cyclopropanation reactions to produce a substituted cyclopropane with different functional groups attached. In this paper, we report transient resonance Raman spectra of a photoproduct formed after ultraviolet excitation of dibromoacetic acid in cyclohexane solution. Comparison of the Raman band vibrational frequencies to those predicted from density functional theory calculations for several probable photoproduct species indicates that noticeable amounts of the iso-dibromoacetic acid product are formed. We compare the properties of iso-dibromoacetic acid to those of the closely related iso-dibromomethane (CH_2Br–Br) species and briefly discuss the possibility for using iso-dibromoacetic acid in cyclopropanation reactions to make substituted cyclopropanes.

Experiment and Calculations

$CHBr_2COOH$ (99%) and spectroscopic grade cyclohexane solvent (99.9+%) were used to prepare samples with concentrations of about 0.10 M to 0.20 M for use in the transient resonance Raman experiments. The experimental apparatus and methods for the transient resonance Raman experiments have been described previously and only a short account will be given here.[11–15,18] The fourth harmonic (266 nm) and the second anti-Stokes hydrogen Raman shifted laser line (368.9 nm) of the second harmonic (532 nm) of a pulsed nanosecond Nd : YAG laser supplied the pump and probe excitation wavelengths for the transient Raman experiments. An optical time delay of about 5 ns was used between the pump and probe laser pulses and a near collinear geometry was used to excite a flowing liquid stream of sample. A backscattering geometry was used to collect the Raman scattered light which was subsequently imaged through a depolarizer and entrance slit of a 0.5 m spectrograph. The grating of the spectrograph dispersed the Raman light onto a liquid nitrogen cooled CCD detector which accumulated the Raman signal for about 300s before being read out to an interfaced PC computer. Approximately 10 to 15 of these readouts were summed to obtain a Raman spectrum. The known Raman band frequencies of cyclohexane were used to calibrate the Raman shifts of the spectra. The transient resonance Raman spectrum was obtained by subtracting the probe only spectrum from the pump–probe spectrum in order to remove parent and solvent Raman bands.

All of the density functional theory (DFT) calculations presented in this paper were done using the Gaussian program suite (G98W).[31] Complete geometry optimizations were done using C1 symmetry and the B3LYP method.[32–34] Vibrational frequencies were also computed at the optimized geometry for the chemical species of interest. The Sadlej-pVTZ basis set was used for the B3LYP computations.[35,36]

Results and Discussion

Figure 1 presents a typical pump-only spectrum in the probe wavelength region (A), a probe only resonance Raman spectrum (B), a pump–probe resonance Raman spectrum (C) and a transient resonance Raman spectrum (D) of the photoproduct produced after 266 nm photolysis of dibromoacetic acid in cyclohexane solution. The transient resonance Raman spectrum was obtained after subtraction of the probe only spectrum from the pump–probe spectrum. Fig. 2 shows an expanded view of the transient resonance Raman spectrum of the dibromoacetic acid photoproduct species. Inspection of Fig. 2 shows that most of the Raman intensity appears in seven bands at 174 cm^{-1}, 614 cm^{-1}, 659 cm^{-1}, 742 cm^{-1}, 834 cm^{-1}, 982 cm^{-1}, 1287 cm^{-1} and several others at 327 cm^{-1}, 1234 cm^{-1} and 1645 cm^{-1}. Table 1 lists the Raman shifts of these bands.

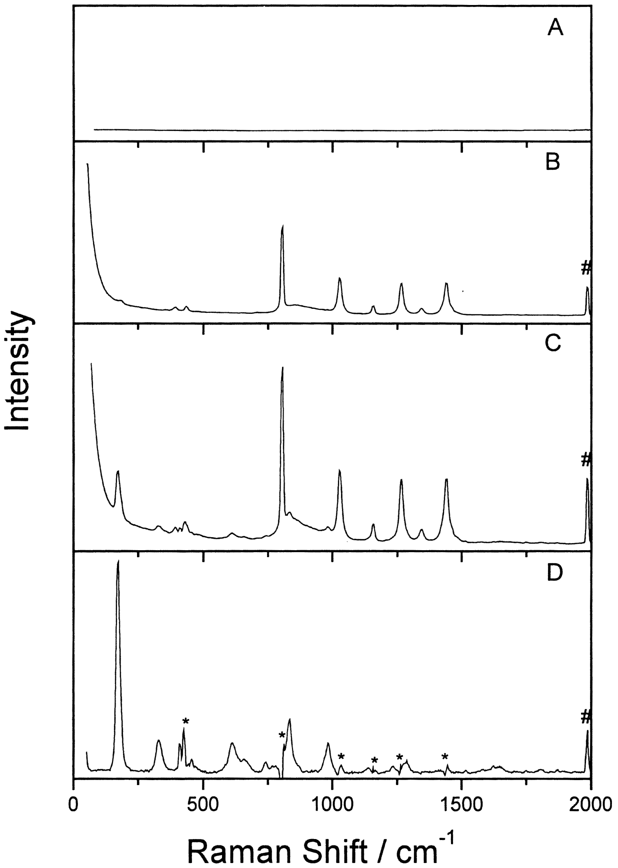

Fig. 1. A typical pump only spectrum in the probe wavelength region (A), a probe only spectrum (B) and a pump–probe spectrum (C) are shown for dibromoacetic acid in cyclohexane solvent. A transient resonance Raman spectrum (D) was obtained by subtracting a probe only spectrum and a pump only spectrum from the pump–probe spectrum. The pump and probe excitation wavelengths were 266 nm and 368.9 nm respectively. The time delay between the pump and probe wavelengths was ~5 ns. The asterisks (*) mark sections where solvent/parent band subtraction artifacts are present and the pound signs (#) label stray light artifacts.

We have employed density functional theory (DFT) calculations to obtain the optimized geometries and vibrational frequencies for several probable photoproduct species (iso-dibromoacetic acid, bromoacetic acid radical and dibromoacetic acid cation) formed after ultraviolet photolysis of dibromoacetic acid in cyclohexane solution. Table 2 lists the optimized geometries for iso-dibromoacetic acid (Br–BrCHCOOH), the bromoacetic acid radical (BrCHCOOH) and the dibromoacetic acid cation ($\mathrm{Br_2CHCOOH^+}$) species found from the B3LYP/Sadlej-pVTZ calculations. Table 3 compares the experimental vibrational frequencies found from the transient resonance Raman spectrum shown in Fig. 2 with those predicted from the B3LYP/Sadlej DFT calculations for several probable photoproduct species. Examination of Table 3 shows that the transient resonance Raman vibrational frequencies agree well with those for the iso-dibromoacetic acid (Br–BrCHCOOH) photoproduct but not with those predicted for the bromoacetic acid radical (BrCHCOOH) and the dibromoacetic acid cation ($\mathrm{Br_2CHCOOH^+}$) species. For example, the BrCHCOOH radical has no calculated vibrational frequencies in the 600–700 cm^{-1} region that would correspond to the experimental Raman bands observed at 614 cm^{-1} and 659 cm^{-1}. The BrCHCOOH radical also has no computed vibrational frequencies in the 800–900 cm^{-1} region that would correspond to the experimental Raman band at 834 cm^{-1}. This indicates that the transient resonance Raman spectrum of the photoproduct is not due to the BrCHCOOH radical. Similarly, the $\mathrm{Br_2CHCOOH^+}$ cation has no predicted vibrational frequencies in the 1250 to 1350 cm^{-1} region that would correspond to the experimental Raman band at 1287 cm^{-1}. In addition, the $\mathrm{Br_2CHCOOH^+}$ cation predicted vibrational frequencies 142 cm^{-1}, 694 cm^{-1}, 775 cm^{-1}, 930 cm^{-1}, 1102 cm^{-1} and 1198 cm^{-1} are more than 30 cm^{-1} away from the experimental bands observed at 174 cm^{-1}, 659 cm^{-1}, 742 cm^{-1}, 834 cm^{-1}, 982 cm^{-1}, and 1140 cm^{-1}. This suggests that the transient resonance Raman spectrum shown in Fig. 2 is not due to the $\mathrm{Br_2CHCOOH^+}$ cation. The transient resonance Raman spectrum shown in Fig. 2 is attributed to the iso-dibromoacetic acid (Br–BrCHCOOH) species and the Raman bands are assigned as follows: the 174 cm^{-1} fundamental

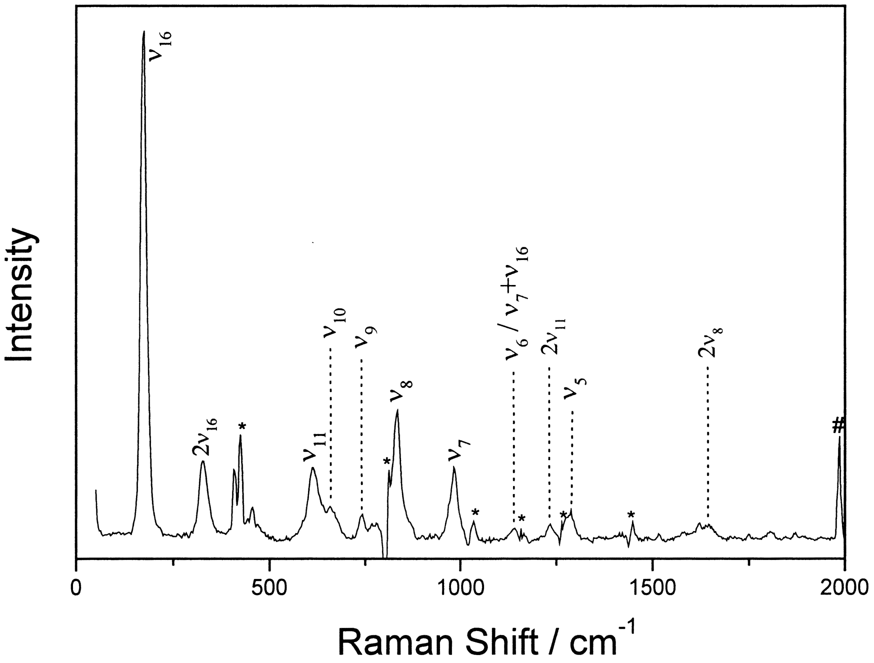

Fig. 2. An expanded view of the transient resonance Raman spectrum of the dibromoacetic acid photoproduct obtained using 266 nm pump and 389.9 nm probe excitation wavelengths and a time delay of ~5 ns. The larger Raman bands are labeled with their tentative assignments (see text and Tables 1 and 3 for more details). The asterisks (*) mark sections where solvent/parent band subtraction artifacts are present and the pound signs (#) label stray light artifacts.

Table 1. Vibrational Frequencies and Preliminary Assignments to the Iso-dibromoacetic Acid Photoproduct (See Text for More Details) for the Larger Raman Bands Observed in the Transient Resonance Raman Spectrum Shown in Fig. 2

Preliminary assignment	Vibrational frequency/cm^{-1}
ν_{16}	174
$2\nu_{16}$	327
ν_{11}	614
ν_{10}	659
ν_9	742
ν_8	834
ν_7	982
ν_6 and/or $\nu_7 + \nu_{16}$	1140
$2\nu_{11}$	1234
ν_5	1287
$2\nu_8$	1645

to the nominal Br–Br stretch mode ν_{16} (calculated to be at 167 cm^{-1}), the 614 cm^{-1} fundamental to the nominal O=C–O bend mode ν_{11} (calculated to be at 617 cm^{-1}), the 659 cm^{-1} fundamental to the nominal C–H wag mode ν_{10} (calculated to be at 655 cm^{-1}), the 742 cm^{-1} fundamental to the nominal C–C wag mode ν_9 (calculated to be at 757 cm^{-1}), the 834 cm^{-1} fundamental to the nominal C–Br stretch mode ν_8 (computed to be at 833 cm^{-1}), the 982 cm^{-1} fundamental to the nominal C–Br and C–C stretch mode ν_7 (computed to be at 988 cm^{-1}), the 1140 cm^{-1} fundamental to the nominal C–O stretch and C–H wag mode ν_6 (computed to be at 1124 cm^{-1}), and the 1287 cm^{-1} fundamental to the nominal C–H and O–H wag mode ν_5 (calculated to be at 1257 cm^{-1}). Table 1 displays the Raman shifts of the bands observed in Fig. 2 and shows their preliminary assignments. Our results indicate the transient resonance Raman spectrum observed in Fig. 2 is due mainly to the iso-dibromoacetic acid (Br–BrCHCOOH) species formed after ultraviolet photolysis of dibromoacetic acid in cyclohexane solution. This is similar to the observation of the iso-dibromomethane (CH_2Br–Br) species observed by transient resonance Raman spectroscopy following ultraviolet pholoysis of CH_2Br_2 in cyclohexane solution.[14,15]

It is interesting to compare the properties of the iso-dibromoacetic acid (Br–BrCHCOOH) species to those of the closely related iso-dibromomethane (CH_2Br–Br) species. The C–Br bond length, the Br–Br bond length, and the C–Br–Br bond angle of the iso-dibromoacetic acid (Br–BrCHCOOH) species (1.778/Å, 2.656/Å, and 118.9/degrees respectively) are close to the values found for the iso-dibromomethane (CH_2Br–Br) species (1.768/Å, 2.674/Å, and 122.0/degrees respectively). This suggests that the chemical reactivity of the CHBr–Br part of the iso-dibromoacetic acid (Br–BrCHCOOH) species is likely similar to that of the CH_2Br–Br species. Previous DFT calculations[15,30] have shown that CH_2Br–Br can readily react with ethylene to form cyclopropane and a Br_2 leaving group with a barrier to reaction of ~6 to 7 kcal/mol. The photolysis of dibromomethane (CH_2Br_2) in the presence of olefins has also shown to form cyclopropanated product experimentally similar to photolysis of diiodomethane in the presence of olefins.[7–10] Thus, it may be possible for the iso-dibromoacetic acid (Br–BrCHCOOH) species to exhibit carbenoid behavior towards olefins and produce a substituted cyclopropanated product (addition of a CHCOOH group to the C=C bond). Further work is needed to determine the actual carbenoid be-

Table 2. Parameters for the Optimized Geometries Computed from the B3LYP/Sadlej-pVTZ Calculations for Iso-dibromoacetic Acid (Br–BrCHCOOH), the Bromoacetic Acid Radical (BrCHCOOH) and the Dibromoacetic Acid Cation ($Br_2CHCOOH^+$) species (Bond Lengths Are in Å Units and Bond Angles Are in Degrees Units)

Parameter	B3LYP/Sadlej-pVTZ	Parameter	B3LYP/
Iso-dibromoacetic acid (Br–BrCHCOOH)		**Iso-dibromomethane (CH_2Br–Br)**	
C–Br	1.778		B3LYP/Aug-pVTZ (from Ref. 14)
Br–Br	2.656	C–Br$_1$	1.768
C–C	1.472	Br$_1$–Br$_2$	2.674
C=O	1.212	C–H$_3$ and C–H$_4$	1.078
C–O	1.3565	C–Br$_1$–Br$_2$	122.0
O–H	0.973	Br$_1$–C–H$_3$ and Br$_1$–C–H$_4$	118.1
C–H	1.091	H$_3$–C–Br$_1$–Br$_2$	−80.68
Br–Br–C	118.9	H$_4$–C–Br$_1$–Br$_2$	80.68
C–C–Br	119.95		
C–C=O	126.2		
C–C–O	109.9		
C–C–H	121.3		
C–O–H	106.9		
O=C–O	123.9		
Br–C–H	117.6		
D(C–C–Br–Br)	85.0		
D(H–C–Br–Br)	−82.7		
D(Br–C–C=O)	1.7		
D(Br–C–C–O)	−179.5		
D(H–C–C=O)	168.8		
D(H–C–C–O)	−12.4		
D(C–C–O–H)	−178.1		
D(O=C–O–H)	0.7		
Bromoacetic acid radical (BrCHCOOH)		**Dibromoacetic acid cation ($Br_2CHCOOH^+$)**	
C–Br	1.856		B3LYP/Sadlej-pVTZ
C–C	1.451	C–Br$_1$	1.997
C=O	1.223	C–Br$_2$	1.904
C–O	1.353	C–C	1.513
O–H	0.972	C–O	1.298
C–H	1.0895	C=O	1.2355
C–C–Br	124.4	O–H	0.981
C–C=O	121.5	C–H	1.0995
C–C–O	115.2	C–C–Br$_1$	98.9
C–C–H	118.8	Br$_1$–C–Br$_2$	112.9
C–O–H	106.4	Br$_1$–C–H	106.8
D(C–C–O–H), D(O–C–C–H) and D(O=C–C–Br)	180.0	Br$_2$–C–H	109.7
		C–C–Br$_2$	116.6
D(O–C–C–Br)	0.0	C–C–H	111.2
		C–C–O	117.3
		C–C=O	116.8
		C–O–H	112.4
		D(Br$_1$–C–C–O)	−174.2
		D(Br$_1$–C–C=O)	7.6
		D(Br$_2$–C–C–O)	−52.9
		D(Br$_2$–C–C=O)	128.9
		D(H–C–C–O)	73.8
		D(C–C–O–H)	−178.4

havior of iso-dibromoacetic acid and its potential use for synthesis of substituted cylopropanated products.

This work was supported by grants to DLP from the Research Grants Council (RGC) of Hong Kong (HKU 7087/01P), the Committee on Research and Conference Grants (CRCG) from the University of Hong Kong, and the Large Items of Equipment Allocation 1993–94 from the University of Hong Kong.

Table 3. Comparison of the Experimental Vibrational Frequencies (in /cm^{-1}) Obtained from the Transient Resonance Raman Spectra (This Work) to the B3LYP/Sadlej-pVTZ Density Functional Theory Calculated Vibrational Frequencies

Vibrational mode	B3LYP/Sadlej-pVTZ Calcd freq./cm^{-1}	Transient Raman Expt freq./cm^{-1}
Iso-dibromoacetic acid (Br–BrCHCOOH)		
ν_1, O–H stretch	3752	
ν_2, C–H stretch	3209	
ν_3, C=O and C–C stretch	1777	
ν_4, C–O and C–Br stretch	1385	
ν_5, C–H and O–H wag	1257	1287
ν_6, C–O stretch and C–H wag	1124	1140
ν_7, C–Br and C–C stretch	988	982
ν_8, C–Br stretch	833	834
ν_9, C–C wag i.p.	757	742
ν_{10}, C–H wag	655	659
ν_{11}, O=C–O bend	617	614
ν_{12}, O–H wag	556	
ν_{13}, C–O wag	375	
ν_{14}, C–C–Br wag	205	
ν_{15}, C–C wag o.p.	193	
ν_{16}, Br–Br stretch	167	174
ν_{17}, C=O wag	63	
ν_{18}, C–O–H wag	54	
Bromoacetic acid radical (BrCHCOOH)		
ν_1, O–H stretch	3766	
ν_2, C–H stretch	3227	
ν_3, O–C=O stretch	1704	
ν_4, O–H wag + C–C stretch	1410	
ν_5, C–H wag	1235	
ν_6, O–H wag	1192	
ν_7, C–C stretch and C–O stretch	950	
ν_8, C–C wag	768	
ν_9, C–C wag o.p.	726	
ν_{10}, C–O–H wag	584	
ν_{11}, O–H wag o.p. + C–H wag o.p.	573	
ν_{12}, C–H wag o.p.	531	
ν_{13}, C=O wag	380	
ν_{14}, C–O wag	179	
ν_{15}, C–H wag o.p.	117	
Dibromoacetice acid cation ($Br_2CHCOOH^+$)		
ν_1, O–H stretch	3663	
ν_2, C–H stretch	3111	
ν_3, O=C–O asym. stretch	1619	
ν_4, C–C stretch	1460	
ν_5, C–H wag and O–H wag	1206	
ν_6, C–H wag and O–H wag	1198	
ν_7, C–H wag	1102	
ν_8, C–C stretch	930	
ν_9, C–Br_2 stretch and C–C wag	775	
ν_{10}, Br–C–Br asym stretch	695	
ν_{11}, O–H wag	634	
ν_{12}, O=C–O bend	586	
ν_{13}, C–C and O–H wag	472	
ν_{14}, C–Br_1 stretch	351	
ν_{15}, Br–C–Br wag	227	
ν_{16}, C–C wag	142	
ν_{17}, Br–C–Br bend	106	
ν_{18}, O=C–O wag	62	

Table 3. (Continued)

Iso-dibromomethane ($CH_2Br–Br$)

		B3LYP/Aug-pVTZ (from Ref. 14)	Transient Raman (from Ref. 14)
A′	ν_1, CH_2 sym stretch	3152	
	ν_2, CH_2 scissor	1428	
	ν_3, C–Br stretch	858	
	ν_4, CH_2 wag	738	690
	ν_5, Br–Br stretch	180	176
	ν_6, C–Br–Br bend	133	146
A″	ν_7, CH_2 asym stretch	3286	
	ν_8, CH_2 rock	966	960
	ν_9, CH_2 twist	468	480*

References

1 Th. Class and K. Ballschmiter, *J. Atmos. Chem.*, **6**, 35 (1988).

2 S. Klick and K. Abrahamsson, *J. Geophys. Res. [Oceans]*, **97**, 12683 (1992).

3 J. C. Mössigner, D. E. Shallcross, and R. A. Cox, *J. Chem. Soc., Faraday Trans.*, **94**, 1391 (1998).

4 C. T. McElroy, C. A. McLinden, and J. C. McConnell, *Nature*, **397**, 338 (1999).

5 L. J. Carpenter, W. T. Sturges, S. A. Penkett, and P. S. Liss, *J. Geophys. Res. [Atmos]*, **104**, 1679 (1999).

6 B. Alicke, K. Hebstreit, J. Stutz, and U. Platt, *Nature*, **397**, 572 (1999).

7 D. C. Blomstrom, K. Herbig, and H. E. Simmons, *J. Org. Chem.*, **30**, 959 (1965).

8 N. J. Pienta and P. J. Kropp, *J. Am. Chem. Soc.*, **100**, 655 (1978).

9 P. J. Kropp, N. J. Pienta, J. A. Sawyer, and R. P. Polniaszek, *Tetrahedron*, **37**, 3229 (1981).

10 P. J. Kropp, *Acc. Chem. Res.*, **17**, 131 (1984).

11 X. Zheng and D. L. Phillips, *J. Phys. Chem. A*, **104**, 6880 (2000).

12 X. Zheng and D. L. Phillips, *Chem. Phys. Lett.*, **324**, 175 (2000).

13 X. Zheng and D. L. Phillips, *J. Chem. Phys.*, **113**, 3194 (2000).

14 X. Zheng, W. M. Kwok, and D. L. Phillips, *J. Phys. Chem. A*, **104**, 10464 (20000).

15 X. Zheng, W.-H. Fang, and D. L. Phillips, *J. Chem. Phys.*, **113**, 10934 (2000).

16 W. M. Kwok, C. Ma, A. W. Parker, D. Phillips, M. Towrie, P. Matousek, and D. L. Phillips, *J. Chem. Phys.*, **113**, 7471 (2000).

17 W. M. Kwok, C. Ma, A. W. Parker, D. Phillips, M. Towrie, P. Matousek, X. Zheng, and D. L. Phillips, *J. Chem. Phys.*, **114**, 7536 (2001).

18 X. Zheng, C. W. Lee, Y.-L. Li, W.-H. Fang, and D. L. Phillips, *J. Chem. Phys.*, **114**, 8347 (2001).

19 B. J. Schwartz, J. C. King, J. Z. Zhang, and C. B. Harris, *Chem. Phys. Lett.*, **203**, 503 (1993).

20 K. Saitow, Y. Naitoh, K. Tominaga, and Y. Yoshihara, *Chem. Phys. Lett.*, **262**, 621 (1996).

21 A. N. Tarnovsky, J.-L. Alvarez, A. P. Yartsev, V. Sündstrom, and E. Åkesson, *Chem. Phys. Lett.*, **312**, 121 (1999).

22 A. N. Tarnovsky, M. Wall, M. Rasmusson, T. Pascher, and E. Åkesson, *J. Chin. Chem. Soc.*, **47**, 769 (2000).

23 W. M. Kwok, C. Ma, A. W. Parker, D. Phillips, M. Towrie, P. Matousek, and D. L. Phillips, *Chem. Phys. Lett.*, **341**, 292 (2001).

24 G. Maier and H. P. Reisenauer, *Angew. Chem., Int. Ed. Engl.*, **25**, 819 (1986).

25 G. Maier, H. P. Reisenauer, J. Hu, B. A. Hess Jr., and L. J. Schaad, *Tetrahedron Lett.*, **30**, 4105 (1989).

26 G. Maier, H. P. Reisenauer, J. Lu, L. J. Schaad, and B. A. Hess Jr., *J. Am. Chem. Soc.,* **112**, 5117 (1990).

27 Ref. 17 (unpublished results) of G. Maier, H. P. Reisenauer, J. Lu, L. J. Schaad, and B. A. Hess Jr., *J. Am. Chem. Soc.*, **112**, 5117 (1990).

28 D. L. Phillips, W. H. Fang, and X. Zheng, *J. Am. Chem. Soc.*, **123**, 4197 (2001).

29 Y. L. Li, K. H. Leung, and D. L. Phillips, *J. Phys. Chem. A*, **105**, 10621 (2001).

30 D. L. Phillips and W. H. Fang, *J. Org. Chem.*, **66**, 5890 (2001).

31 M. J. Frisch, G. W. Trucks, H. B. Schlegel, G. E. Scuseria, M. A. Robb, J. R. Cheeseman, V. G. Zakrzewski, J. A. Montgomery, Jr., R. E. Stratmann, J. C. Burant, S. Dapprich, J. M. Millam, A. D. Daniels, K. N. Kudin, M. C. Strain, O. Farkas, J. Tomasi, V. Barone, M. Cossi, R. Cammi, B. Mennucci, C. Pomelli, C. Adamo, S. Clifford, J. Ochterski, G. A. Petersson, P. Y. Ayala, Q. Cui, K. Morokuma, D. K. Malick, A. D. Rabuck, K. Raghavachari, J. B. Foresman, J. Cioslowski, J. V. Ortiz, A. G. Baboul, B. B. Stefanov, G. Liu, A. Liashenko, P. Piskorz, I. Komaromi, R. Gomperts, R. L. Martin, D. J. Fox, T. Keith, M. A. Al-Laham, C. Y. Peng, A. Nanayakkara, C. Gonzalez, M. Challacombe, P. M. W. Gill, B. Johnson, W. Chen, M. W. Wong, J. L. Andres, C. Gonzalez, M. Head-Gordon, E. S. Replogle, and J. A. Pople, "Gaussian 98, Revision A. 7," Gaussian, Inc., Pittsburgh PA (1998).

32 A. D. Becke, *Phys. Rev. A*, **38**, 3098 (1988).

33 A. D. Becke, *J. Chem. Phys.*, **98**, 1372 (1993).

34 C. Lee, W. Yang, and R. G. Parr, *Phys. Rev. B*, **58**, 785 (1988).

35 A. J. Sadlej, *Theor. Chim. Acta*, **79**, 123 (1992).

36 A. J. Sadlej, *Theor. Chim. Acta*, **81**, 339 (1992).